



OPEN

The atypical E2F transcription factor DEL1 modulates growth–defense tradeoffs of host plants during root-knot nematode infection

Satoru Nakagami¹, Kentaro Saeki¹, Kei Toda¹, Takashi Ishida^{1,2} & Shinichiro Sawa¹✉

In plants, growth–defense tradeoffs are essential for optimizing plant performance and adaptation under stress conditions, such as pathogen attack. Root-knot nematodes (RKNs) cause severe economic losses in many crops worldwide, although little is known about the mechanisms that control plant growth and defense responses during nematode attack. Upon investigation of *Arabidopsis thaliana* infected with RKN (*Meloidogyne incognita*), we observed that the atypical transcription factor *DP-E2F-like 1 (DEL1)* repressed salicylic acid (SA) accumulation in RKN-induced galls. The *DEL1*-deficient *Arabidopsis* mutant (*del1-1*) exhibited excessive SA accumulation in galls and is more resistant to RKN infection. In addition, excessive lignification was observed in galls of *del1-1*. On the other hand, the root growth of *del1-1* is reduced after RKN infection. Taken together, these findings suggest that *DEL1* plays an important role in the balance between plant growth and defense responses to RKN infection by controlling SA accumulation and lignification.

Salicylic acid (SA) is a key plant defense hormone required for immunity against pathogen infection¹. Pathogens often induce SA accumulation both locally and systemically. This pathogen-induced SA is synthesized through the isochorismate pathway comprised of ISOCHORISMATE SYNTHASE 1 (ICS1), ENHANCED DISEASE SUSCEPTIBILITY 5 (EDS5), and *avrPphB* SUSCEPTIBLE 3 (PBS3)². A recent study has revealed that ICS1, EDS5 and PBS3 are necessary for pathogen-induced SA biosynthesis in plants². SA accumulation leads to the activation of plant defense responses, including programmed cell death and systemic acquired resistance. High levels of SA accumulation result in changes in transcriptional activities of genes with antimicrobial activity such as the *PATHOGENESIS-RELATED (PR)* genes³. In *Arabidopsis thaliana*, SA-dependent transcriptional reprogramming requires NONEXPRESSER OF PR GENES 1 (NPR1), which was shown to be the *bona fide* SA receptor and also functions as a transcriptional co-activator⁴. Many studies have reported SA-induced defense responses upon infection by leaf-colonizing pathogens⁵, while little is known about the involvement of SA-induced defense responses in roots.

Several studies have shown that SA metabolism is also targeted by phytoparasitic root-knot nematodes (RKNs; *Meloidogyne* spp.) to ensure successful infection⁶. RKNs cause severe yield losses of many crop species in multiple regions of the world⁷. During RKN infections, juveniles invade plant roots and move toward the vascular cylinder. Upon reaching the vascular cylinder, RKNs induce the formation of galls, each containing several giant cells (GCs) which serve as a source of nutrients for the nematode until maturity. Since GCs result from nuclear divisions without cytokinesis (endoreduplication), it is thought that RKN is capable of manipulating the host cell-cycle machinery⁶. Biotrophic pathogens such as RKNs must keep the host cells alive while also suppressing host defense mechanisms. Repression of genes of the SA pathway was indeed observed in RKN-induced galls^{8–10}. In addition, overexpression of *NPR1* leads to the decrease in the number of galls and RKN fecundity during RKN infection¹¹. On the other hand, overexpression of SA-degrading salicylate hydroxylase leads to reduced SA accumulation and greater susceptibility to RKN¹².

¹Graduate School of Science and Technology, Kumamoto University, Kumamoto, 860-8555, Japan. ²International Research Organization for Advanced Science and Technology (IROAST), Kumamoto University, Kumamoto, 860-8555, Japan. ✉e-mail: sawa@kumamoto-u.ac.jp

SA accumulation contributes to plant defense responses, while excessive SA often leads to growth inhibition. Therefore, it is generally believed that host plants must balance growth and defense during pathogen infection. How this is accomplished is currently unknown. The Arabidopsis atypical transcription factor *DP-E2F-like 1* (*DEL1*)/*E2Fe*, a transcriptional repressor known to promote the onset of endoreduplication, has been shown to balance plant growth and defense via the SA response in leaves during pathogenic fungi infection¹³. Here, we report that *DEL1* represses excessive SA accumulation and root growth inhibition of host plants upon RKN infection. Furthermore, lignin deposition was also shown to be elevated in galls of the *del1-1* knockout mutant. Our results suggest that *DEL1* plays a role in balancing growth and defense in roots as previously reported in leaves¹³.

Results

SA biosynthesis is enhanced in *del1-1* galls. Chandran *et al.* showed that *DEL1* acts as a transcriptional repressor of *EDS5*¹³. The enhanced resistance to fungi and the small stature phenotypes of *del1-1* were shown to be SA-dependent. *DEL1*-mediated SA accumulation has been demonstrated in leaves¹³, but it is unclear whether plants also balance growth–defense tradeoffs in the roots. To address this question, we subjected *del1-1* to the RKN infection assay. We performed reverse transcription quantitative polymerase chain reaction (RT-qPCR) on genes related to SA biosynthesis in wild-type (WT) and *del1-1* galls. *EDS5* and *PBS3* were up-regulated in the galls of *del1-1* compared to the WT, while *ICS1* did not show significant difference between transcript levels in *del1-1* and WT galls (Fig. 1A). We next tested whether SA accumulation in *del1-1* galls was higher than that in WT galls. Indeed, total SA accumulation in *del1-1* galls was significantly higher than that in WT galls (Fig. 1B). On the other hand, total SA level in un-inoculated roots of *del1-1* did not change significantly compared to that of WT (Fig. 1B). These results showed that *DEL1* represses SA biosynthesis in RKN-induced galls.

Gall formation is compromised in *del1-1*. To determine whether the elevated SA levels activate the defense response, we analyzed the expression of the SA-dependent genes *PR1*, *PR2*, *PR5* and *NPR1* in galls. *PR1* transcripts were not detected from the galls of neither WT nor *del1-1* (Fig. S1), suggesting that *PR1* is likely not involved in RKN infection. On the other hand, *PR2* and *PR5* were up-regulated in the galls of *del1-1* compared to the WT, whereas *NPR1* expression level did not change (Fig. S1). These results suggest transcript level of *PR2* and *PR5* may be modified by SA accumulation in the galls of *del1-1*. Previous studies have shown that SA signaling confers increased host plant resistance to nematode infection^{11,12,14,15}. To examine the functions of *DEL1* in RKN-induced gall formation, we assayed gall formation frequencies and GC formation in *del1-1*. Gall numbers were reduced in the *del1-1* mutant compared to that in the WT (Fig. 2A). Furthermore, histological analysis showed that GC areas were significantly reduced in *del1-1* at 14 days post inoculation (dpi) by approximately one third of the WT value (Figs. 2B and S2), which is consistent with the results from a previous study¹⁶. These results suggest that excessive SA accumulation from the loss-of-function of *del1-1* mutation renders the host plant more resistant to RKN infection. Therefore it is possible that the endocycle machinery itself is involved in the RKN infection together with SA signaling, as de Almeida Engler *et al.* (2019) has shown that *del1-1* mutant with defect of the endocycle machinery produced malformed giant cells¹⁶.

***DEL1* is involved in lignin deposition during RKN infection.** In Arabidopsis roots, cell wall lignification is restricted to the xylem and the Casparian strip during normal development¹⁷. Lignin contributes to the protection of plants from physical and chemical stresses, including pathogen challenges. Several studies have revealed that lignification can affect parasitic nematode infection rates^{18–21}. Galls during early stages were subjected to phloroglucinol-HCl staining to detect lignin, which was weakly stained in 3 dpi galls but became more prominent in 5 dpi galls in WT (Fig. 3A). In contrast, lignin was strongly stained in both 3 dpi and 5 dpi galls of *del1-1* (Fig. 3A). In fact, 5 dpi galls of *del1-1* showed stronger lignin staining than WT galls at 5 dpi (Fig. 3A). Non-galling parts of RKN-infected seedlings in both WT and *del1-1* plants did not show lignin staining except for the vascular tissues (Fig. 3A). Next, we analyzed the transcript levels of lignin biosynthesis-related genes in galls by RT-qPCR. The expression levels of 4-coumarate: CoA ligase 1 (*4CL1*), *4CL2*, alcohol dehydrogenase 5 (*CAD5*), phenylalanine ammonia-lyase 1 (*PAL1*), *PAL2*, and cinnamate 4-hydroxylase (*C4H*) were significantly up-regulated in *del1-1* galls compared to WT galls (Fig. 3B). These results indicate that *DEL1* negatively regulates local lignin deposition during RKN infection.

***del1-1* exhibits root growth inhibition after RKN infection.** Chandran *et al.* (2014) showed that *DEL1* controls rosette leaf size upon pathogen infection, while SA accumulation and lignin deposition are often associated with inhibition of growth in Arabidopsis^{13,22–27}. We therefore questioned whether *DEL1* controls the balance between root growth and immunity after RKN infection. 10-day-old un-inoculated *del1-1* seedlings did not show significant differences in root growth compared to WT (Fig. 4A,B), whereas the total root length of RKN-inoculated *del1-1* seedlings at 7 dpi was significantly reduced compared to WT (Fig. 4A,C). These results indicate that *DEL1* plays an important role in the balancing growth–defense tradeoffs in root during RKN-infection (Figs. 2 and 4).

Discussion

In plants, the activation of immunity is often inversely correlated with growth. Thus, the tradeoff between immunity and growth is thought to be important for survival of plants under biotic stresses. We demonstrated that knocking out *DEL1*/*E2Fe* leads to enhanced resistance and growth inhibition during RKN infection, likely due to excessive lignification and/or SA accumulation in RKN-induced galls (Fig. 5). Our RT-qPCR analysis showed that *PR2* and *PR5* were up-regulated in *del1-1* galls, but *PR1* was not (Fig. S1). This suggests a portion of the SA metabolism genes respond to RKN-induced SA accumulation in *del1-1* galls. Since Fu *et al.* (2012) has shown that *NPR1* protein level is up-regulated post-transcriptionally after SA treatment²⁸, *NPR1* proteins thus are likely to be highly accumulated in *del1-1* galls (Fig. S1). A number of studies have revealed that alterations in lignin biosynthesis

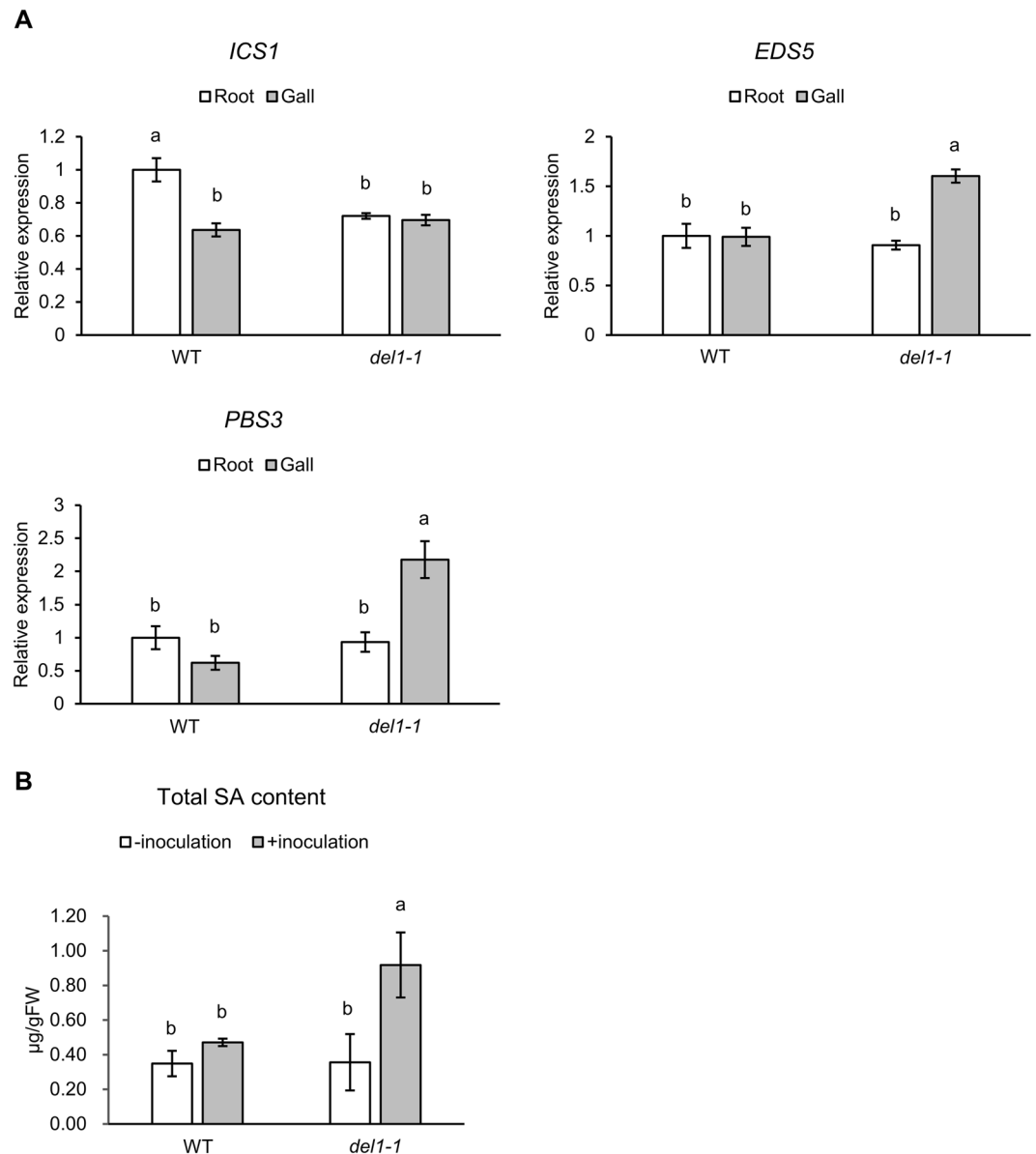


Figure 1. *DEL1* regulates SA biosynthesis during RKN infection. **(A)** RT-qPCR analysis of SA biosynthesis-related genes in WT and *del1-1* galls at 7dpi. Values are normalized to the expression levels in un-inoculated roots of WT. The experiment was repeated three times with similar results. **(B)** Quantification of free and total SA in the WT and the *del1-1* mutant. The experiment was repeated three times with similar results. Means \pm SD are shown. Different letters denote significant differences after Tukey's multiple test at $P < 0.05$.

result in changes in both growth and defense, while excessive lignification inhibits plant growth^{25–27,29}. In addition, transgenic and mutant plants with elevated basal SA levels also exhibit growth reduction^{13,22–24}. Moreover, recent studies have shown that SA accumulation in response to pathogen attack positively correlates with lignin deposition and acquisition of immunity^{30–33}. In light of these lines of evidence, *DEL1* may mediate the balance between defense and growth by limiting SA accumulation during RKN infection in root. Chandran *et al.* (2014) have reported that *del1-1* plants exhibit small rosette leaves and SA accumulation higher than that of WT regardless of fungal infection¹³. On the other hand, our results showed that *del1-1* exhibited root growth inhibition only in the presence of RKN infection (Fig. 4). SA accumulation in roots of *del1-1* in the absence of RKN was not significantly different compared to that of WT (Fig. 1B), suggesting this difference in response between in leaves and in roots may come from differences of SA level in the absence of pathogen infection.

Although reduced parasitic nematode fecundity on *del1-1* has been attributed to the deficiency in cell division during syncytia/gall formation¹⁶, our results point to the additional possibility that the up-regulation of SA accumulation and lignification may also be contributing factors in gall formation efficiency. Further detailed analysis of the function of *DEL1* in SA accumulation/lignification during RKN infection may provide insights into the mechanisms of balancing defense and growth in plants.

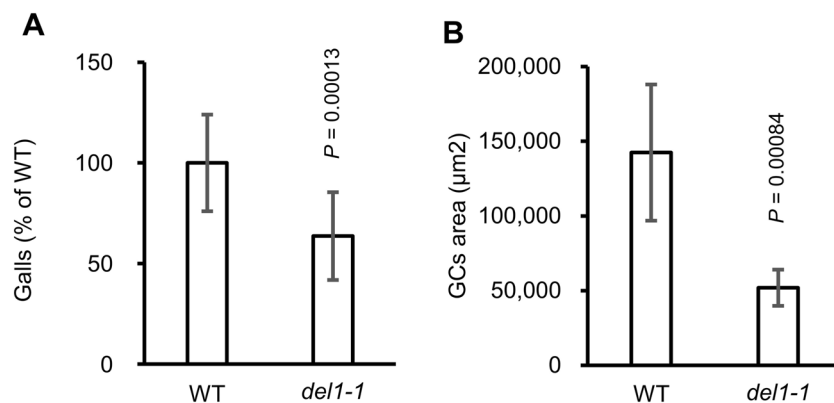


Figure 2. Gall formation is compromised in *del1-1* mutants. **(A)** WT-normalized gall numbers in WT and *del1-1* plants at 7 dpi ($n = 15$, WT; $n = 16$, *del1-1*). Sample sizes denote the number of petri dishes were tested. **(B)** Areas of GCs of 14 dpi galls in WT and *del1-1* plants ($n = 6$). Sample sizes denote the number of galls. Means \pm SD are shown. P values were analyzed by Student's t -test.

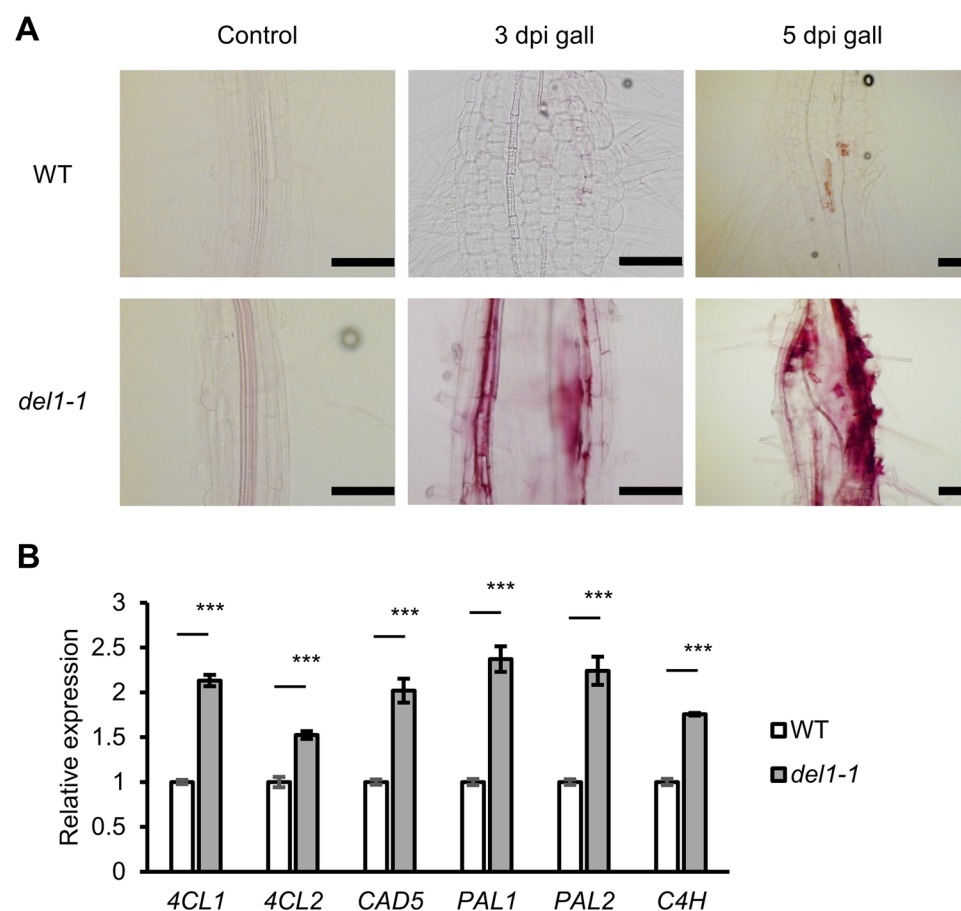


Figure 3. Lignin accumulates specifically in *del1-1* plants after RKN infection. **(A)** Phloroglucinol-HCl staining in non-infected regions of RKN-infected roots (control), 3 dpi and 5 dpi galls (5 individuals were observed with similar results). Top: WT. Bottom: *del1-1*. Scale bars = 100 μm . **(B)** RT-qPCR analysis of lignin synthesis-related genes in WT and *del1-1* 7 dpi galls. Values are normalized to expression levels in the WT. 4CL: 4-coumarate-CoA ligase, CAD: cinnamyl alcohol dehydrogenase, PAL: phenylalanine ammonia-lyase, C4H: cinnamate 4-hydroxylase. The experiment was repeated three times with similar results. Means \pm SD are shown. *** $P < 0.001$ by Student's t -test.

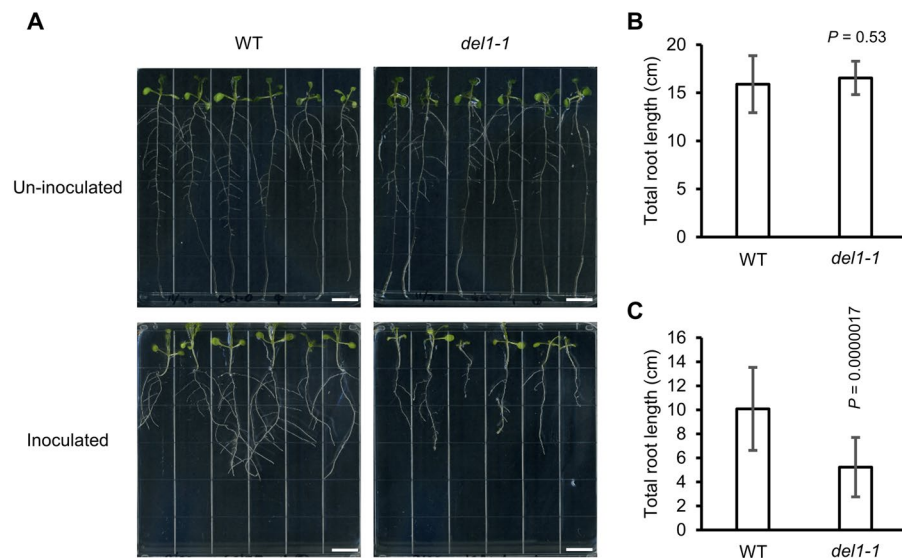


Figure 4. Root growth is inhibited in *del1-1* mutants after RKN infection. **(A)** Representative images of WT and *del1-1* seedlings with or without RKN inoculation. Top: 10-days-old non-inoculated seedlings. Bottom: RKN-inoculated seedlings at 7 dpi. **(B)** Total root length (primary root + lateral roots) of non-inoculated WT and *del1-1* plants ($n = 12$, WT; $n = 11$, *del1-1*). **(C)** Total root length of RKN-inoculated WT and *del1-1* plants ($n = 18$). Means \pm SD are shown. Sample sizes denote the number of plants. The experiment was repeated three times with similar results. *P* values were analyzed by Student's *t*-test.

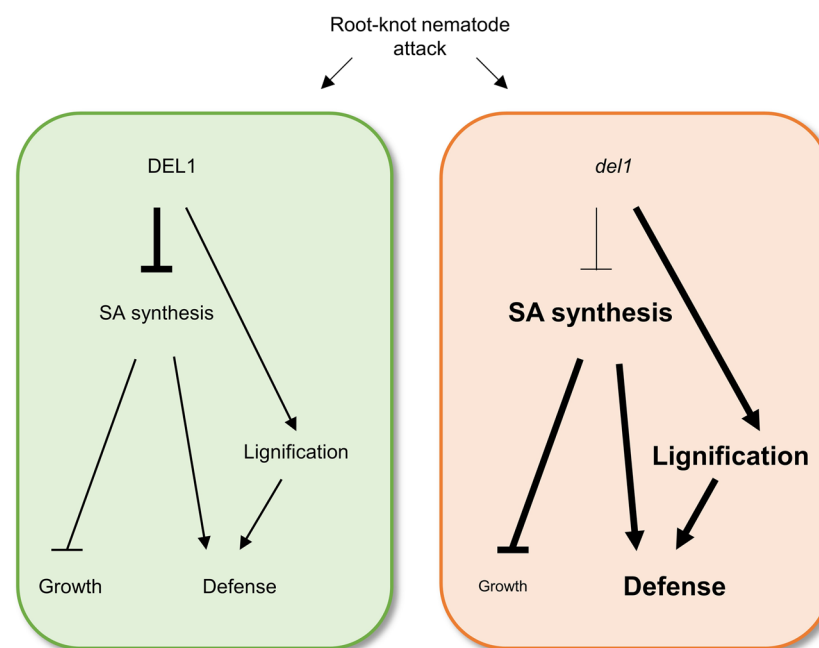


Figure 5. Schematic model depicting the role of *DEL1* during RKN infection. Proposed role for *DEL1* as a mediator plant growth and defense in the RKN infection in Arabidopsis roots. In WT plants, *DEL1* controls basal SA levels and lignification in galls after RKN attack to balance plant growth and defense (green panel). Excessive SA accumulation and lignification due to misexpression of *DEL1* contribute to plant defense after RKN attack, whereas the root growth is inhibited (orange panel).

Methods

Plant materials and growth conditions. All *Arabidopsis thaliana* plants used in this study are of the Col-0 ecotype background. The mutant line, *del1-1*, was obtained from the Arabidopsis Biological Resource Center (ABRC). Arabidopsis seeds were stratified for 2 days in 4 °C in the dark, then allowed to germinate and grown for 5 days on 0.25 \times Murashige and Skoog (MS) salt mixture (Sigma), 0.5% (w/v) sucrose, and 0.6% (w/v) gellan gum at pH 6.4 under continuous light at 23 °C.

Nematode preparation and inoculation. Root-knot nematodes (RKN, *Meloidogyne incognita*) were prepared aseptically as described previously³⁴. Briefly, 6- to 7-week-old tomato plants were inoculated at 3-day intervals for a total of four inoculations. Approximately 80,000 juveniles were used to inoculate each plant. The inoculated tomato plants were then transferred to a hydroponic system, and after 2 to 4 day intervals infective juveniles were collected from the hydroponic culture media. Six *Arabidopsis* seeds were sown on a MS plate. Five-days-old *Arabidopsis* seedlings were inoculated with approximately 80 nematodes per plant and incubated under short-day conditions (8 hours light/16 hours dark) at 25 °C. The roots of the seedlings were covered with black paper to mimic the dark underground environment in nature.

Evaluation of gall formation efficiency. Gall numbers were normalized for each petri dish of six seedlings to evaluate the gall formation efficiency (Data S1). The calculation procedure is as described below: (1) Galls number and germinated seedlings number were counted for each petri dish of six seedlings. (2) Gall number/seedling values were calculated. (3) Average values of galls/seedling in WT were calculated for each independent experiment to define the basal value (highlighted in orange in Data S1). (4) The galls/seedling values from WT and *dell-1* were normalized to the basal value for each petri dish to calculate relative galls number. (5) Average values of relative gall numbers were calculated (highlighted in blue in Data S1). These values were used for Fig. 2A.

Phloroglucinol-HCl staining. Lignin was detected by the Wiesner test by immersing roots or galls of RKN-infected seedlings in phloroglucinol reagent [1% (w/v) phloroglucinol in 20% (v/v) HCl] for 5 minutes. Stained samples were then mounted in chloral hydrate solution (8 g chloral hydrate, 2 ml ultrapure water and 1 ml glycerol). Samples were imaged with an Axio Imager M1 microscope (Carl Zeiss) mounted with a DP71 digital camera (Olympus).

Gene expression analysis. Total RNA was extracted from roots or galls (approximately 50 mg fresh weight) using the RNeasy plant mini kit (Qiagen), then treated with Recombinant DNase I (Takara) according to the manufacturer's instruction. First-strand cDNA was synthesized from 300 ng of total RNA using PrimeScript RT Master Mix (Takara). The transcript level of target genes was assayed using FastStart Essential DNA Green Master (Roche) and the LightCycler 480 system (Roche). The thermal cycler program was 95 °C for 5 min followed by 55 cycles of 95 °C for 10 s, 60 °C for 10 s, and 72 °C for 10 s. *GAPDH* was used as the internal control and relative expression levels were calculated by the $\Delta\Delta C_t$ method. Sequences of primers used are listed in Table S1. Each of the three biological replicates were performed in technical triplicates.

Histological analysis. Galls were dissected and transferred into 2% glutaraldehyde in 20 mM cacodylate buffer, pH 7.4, vacuum-infiltrated for 10 min twice, then incubated in 4 °C overnight. Samples were dehydrated in a graded ethanol series and embedded in Technovit 7100 (Kulzer) according to the manufacturer's protocol. Sample blocks were sectioned to 5 μ m thickness using an ultramicrotome (LEICA RM2255, Leica) and stained with 0.01% (w/v) toluidine blue O (WALDECK) containing 1% (w/v) sodium borate decahydrate (Nacalai) for 2 min. All samples were rinsed in deionized water for 1 min. After drying, sections were mounted in EUKITT (O. Kindler). Samples were imaged with an Axio Imager M1 microscope (Carl Zeiss) mounted with a DP71 digital camera (Olympus). Lengths and areas of the galls were quantified using ImageJ.

Quantification of total SA. Total SA (free SA plus SA glucosides) from *Arabidopsis thaliana* roots was extracted as previously described³⁵. Non-inoculated whole root systems (primary roots and lateral roots) of 12-days-old seedlings, or 7 dpi galls (more than 150 mg fresh weight) were collected. SA of the root exudates was determined by high performance liquid chromatograph–fluorescence detector (HPLC-FL) (LC-2000 plus and FP-2020 plus, Jasco) according to the previous report³⁵. Briefly, 20 μ L of sample was injected in water/methanol (20:80) eluent to be separated from other organic compounds by using a multi-mode column (Scherzo SM-C18, Imtakt, 2 mm \times 50 mm). Fluorescence at 407 nm was monitored with 305 nm excitation for SA and *o*-anisic acid.

Statistical information. All *P* values were derived from two-sided Student's *t*-tests or Tukey's tests. All statistical tests and *n* numbers, including sample sizes or biological replications, are described in the figure legends.

Received: 27 November 2019; Accepted: 6 May 2020;

Published online: 01 June 2020

References

1. Vlot, A. C., Dempsey, D. A. & Klessig, D. F. Salicylic Acid, a multifaceted hormone to combat disease. *Annu. Rev. Phytopathol.* **47**, 177–206 (2009).
2. Rekhter, D. *et al.* Isochorismate-derived biosynthesis of the plant stress hormone salicylic acid. *Science* **365**, 498–502 (2019).
3. Wang, D., Amornsiripanitch, N. & Dong, X. A Genomic Approach to Identify Regulatory Nodes in the Transcriptional Network of Systemic Acquired Resistance in Plants. *PLoS Pathog.* **2**, e123 (2006).
4. Wu, Y. *et al.* The *Arabidopsis* NPR1 Protein Is a Receptor for the Plant Defense Hormone Salicylic Acid. *Cell Rep.* **1**, 639–647 (2012).
5. Palmer, I. A., Shang, Z. & Fu, Z. Q. Salicylic acid-mediated plant defense: Recent developments, missing links, and future outlook. *Front. Biol.* **12**, 258–270 (2017).
6. Favery, B., Quentin, M., Jaubert-Possamai, S. & Abad, P. Gall-forming root-knot nematodes hijack key plant cellular functions to induce multinucleate and hypertrophied feeding cells. *J. Insect Physiol.* **84**, 60–69 (2016).
7. Jones, J. T. *et al.* Top 10 plant-parasitic nematodes in molecular plant pathology: Top 10 plant-parasitic nematodes. *Mol. Plant Pathol.* **14**, 946–961 (2013).
8. Barcala, M. *et al.* Early transcriptomic events in microdissected *Arabidopsis* nematode-induced giant cells. *Plant J.* **61**, 698–712 (2010).

9. Kyndt, T. *et al.* Transcriptional reprogramming by root knot and migratory nematode infection in rice. *N. Phytol.* **196**, 887–900 (2012).
10. Ji, H. *et al.* Transcriptional analysis through RNA sequencing of giant cells induced by *Meloidogyne graminicola* in rice roots. *J. Exp. Botany* **64**, 3885–3898 (2013).
11. Priya, D. B., Somasekhar, N., Prasad, J. & Kirti, P. Transgenic tobacco plants constitutively expressing *Arabidopsis* NPR1 show enhanced resistance to root-knot nematode, *Meloidogyne incognita*. *BMC Res. Notes* **4**, 231 (2011).
12. Nahar, K., Kyndt, T., De Vleeschauwer, D., Höfte, M. & Gheysen, G. The Jasmonate Pathway Is a Key Player in Systemically Induced Defense against Root Knot Nematodes in Rice. *Plant. Physiol.* **157**, 305–316 (2011).
13. Chandran, D. *et al.* Atypical E2F Transcriptional Repressor DEL1 Acts at the Intersection of Plant Growth and Immunity by Controlling the Hormone Salicylic Acid. *Cell Host Microbe* **15**, 506–513 (2014).
14. Molinari, S., Fanelli, E. & Leonetti, P. Expression of tomato salicylic acid (SA)-responsive pathogenesis-related genes in *Mi-1*-mediated and SA-induced resistance to root-knot nematodes: PR genes in genetic and induced resistance to RKNs. *Mol. Plant. Pathol.* **15**, 255–264 (2014).
15. Wubben, M. J. E., Jin, J. & Baum, T. J. Cyst Nematode Parasitism of *Arabidopsis thaliana* Is Inhibited by Salicylic Acid (SA) and Elicits Uncoupled SA-Independent Pathogenesis-Related Gene Expression in Roots. *MPMI* **21**, 424–432 (2008).
16. de Almeida Engler, J. *et al.* CCS52 and DEL1 genes are key components of the endocycle in nematode-induced feeding sites: Endocycle in nematode feeding sites. *Plant. J.* **72**, 185–198 (2012).
17. Barros, J., Serk, H., Granlund, I. & Pesquet, E. The cell biology of lignification in higher plants. *Ann. Bot.* **115**, 1053–1074 (2015).
18. Fujimoto, T., Mizukubo, T., Abe, H. & Seo, S. Sclereol Induces Plant Resistance to Root-Knot Nematode Partially Through Ethylene-Dependent Enhancement of Lignin Accumulation. *MPMI* **28**, 398–407 (2015).
19. Huang, W. K., Ji, H. L., Gheysen, G. & Kyndt, T. Thiamine-induced priming against root-knot nematode infection in rice involves lignification and hydrogen peroxide generation: VB1-induced priming against root-knot nematode. *Mol. Plant. Pathol.* **17**, 614–624 (2016).
20. Veronico, P. *et al.* Changes in lignin biosynthesis and monomer composition in response to benzothiadiazole and root-knot nematode *Meloidogyne incognita* infection in tomato. *J. Plant. Physiol.* **230**, 40–50 (2018).
21. Wuyts, N., Lognay, G., Swennen, R. & De Waele, D. Nematode infection and reproduction in transgenic and mutant *Arabidopsis* and tobacco with an altered phenylpropanoid metabolism. *J. Exp. Botany* **57**, 2825–2835 (2006).
22. Bowling, S. A. *et al.* A mutation in *Arabidopsis* that leads to constitutive expression of systemic acquired resistance. *Plant. Cell* **6**, 1845–1857 (1994).
23. Jirage, D. *et al.* Constitutive salicylic acid-dependent signaling in *cpr1* and *cpr6* mutants requires PAD4. *Plant. J.* **26**, 395–407 (2002).
24. Mauch, F. *et al.* Manipulation of salicylate content in *Arabidopsis thaliana* by the expression of an engineered bacterial salicylate synthase: Manipulation of salicylate content in *Arabidopsis*. *Plant. J.* **25**, 67–77 (2008).
25. Zhong, R., Demura, T. & Ye, Z.-H. SND1, a NAC Domain Transcription Factor, Is a Key Regulator of Secondary Wall Synthesis in Fibers of *Arabidopsis*. *Plant. Cell* **18**, 3158–3170 (2006).
26. Zhong, R., Richardson, E. A. & Ye, Z.-H. The MYB46 Transcription Factor Is a Direct Target of SND1 and Regulates Secondary Wall Biosynthesis in *Arabidopsis*. *Plant. Cell* **19**, 2776–2792 (2007).
27. Zhou, J., Lee, C., Zhong, R. & Ye, Z.-H. MYB58 and MYB63 Are Transcriptional Activators of the Lignin Biosynthetic Pathway during Secondary Cell Wall Formation in *Arabidopsis*. *Plant. Cell* **21**, 248–266 (2009).
28. Fu, Z. Q. *et al.* NPR3 and NPR4 are receptors for the immune signal salicylic acid in plants. *Nature* **486**, 228–232 (2012).
29. Xie, M. *et al.* Regulation of Lignin Biosynthesis and Its Role in Growth-Defense Tradeoffs. *Front. Plant. Sci.* **9**, 1427 (2018).
30. Ma, R. *et al.* AP2/ERF Transcription Factor, *li049*, Positively Regulates Lignan Biosynthesis in *Isatis indigotica* through Activating Salicylic Acid Signaling and Lignan/Lignin Pathway Genes. *Front. Plant. Sci.* **8**, 1361 (2017).
31. Tang, Y. *et al.* Cotton WATs Modulate SA Biosynthesis and Local Lignin Deposition Participating in Plant Resistance Against *Verticillium dahliae*. *Front. Plant. Sci.* **10**, 526 (2019).
32. Yuan, W. *et al.* Maize phenylalanine ammonia-lyases contribute to resistance to *Sugarcane mosaic virus* infection, most likely through positive regulation of salicylic acid accumulation. *Molecular Plant Pathology* 12817 (2019).
33. Zhang, Z. *et al.* Cotton plant defence against a fungal pathogen is enhanced by expanding BLADE-ON-PETIOLE1 expression beyond lateral-organ boundaries. *Commun. Biol.* **2**, 238 (2019).
34. Nishiyama, H. *et al.* Protocol for root-knot nematode culture by a hydroponic system and nematode inoculation to *Arabidopsis*. *Japanese J. Nematology* **45**, 45–49 (2015).
35. Allasia, V. *et al.* Quantification of Salicylic Acid (SA) and SA-glucosides in *Arabidopsis thaliana*. *BIO-PROTOCOL* **8** (2018).

Acknowledgements

We are grateful to Chika Ejima and Hiroshi Sato (Kumamoto University) for technical support, and Allen Yi-Lun Tsai (RIKEN) for critical reading of the manuscript. We are also grateful to ABRC for providing *dell-1* seeds. This research has been funded by KAKENHI Grant Numbers 24114009, 24370024, 16K14757, 17H03967, 18H05487, and 20H00422 to S.S.

Author contributions

S.N.: conceptualization; formal analysis; investigation; project administration; validation; visualization; writing, original draft; writing, review, and editing; K.S.: investigation; K.T.: investigation; validation; T.I.: conceptualization; resources; writing, review, and editing; S.S.: conceptualization; funding acquisition; project administration; supervision; writing, review, and editing.

Competing interests

The authors declare no competing interests.

Additional information

Supplementary information is available for this paper at <https://doi.org/10.1038/s41598-020-65733-3>.

Correspondence and requests for materials should be addressed to S.S.

Reprints and permissions information is available at www.nature.com/reprints.

Publisher's note Springer Nature remains neutral with regard to jurisdictional claims in published maps and institutional affiliations.



Open Access This article is licensed under a Creative Commons Attribution 4.0 International License, which permits use, sharing, adaptation, distribution and reproduction in any medium or format, as long as you give appropriate credit to the original author(s) and the source, provide a link to the Creative Commons license, and indicate if changes were made. The images or other third party material in this article are included in the article's Creative Commons license, unless indicated otherwise in a credit line to the material. If material is not included in the article's Creative Commons license and your intended use is not permitted by statutory regulation or exceeds the permitted use, you will need to obtain permission directly from the copyright holder. To view a copy of this license, visit <http://creativecommons.org/licenses/by/4.0/>.

© The Author(s) 2020